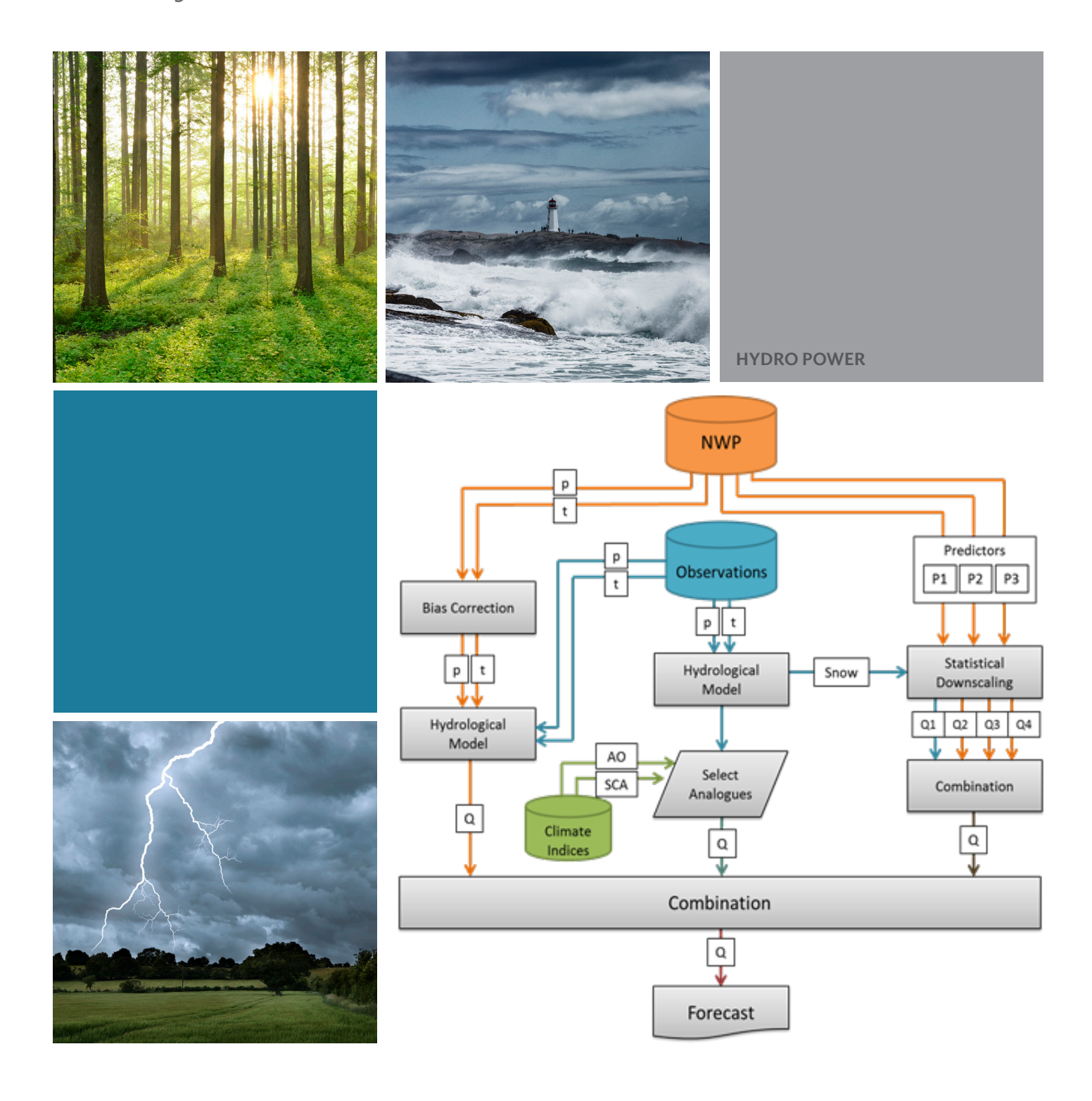
HYDROLOGICAL SEASONAL FORECAST SYSTEM

A PROTOTYPE MULTI-MODEL SYSTEM FOR FORECASTING THE SPRING FLOOD

REPORT 2015:206





Hydrological Seasonal Forecast System

A prototype multi-model system for forecasting the spring flood

KEAN FOSTER, CINTIA UVO, JONAS OLSSON AND JOHAN SÖDLING

Foreword

In this project a prototype multi-model system for forecasting the volumes of the spring flood has been developed and evaluated for selected rivers in northern Sweden. On average the Hydrological Seasonal Forecast System (HSFS) performs better than the operational IHMS forecasts 62% of the time which translates to a 2% reduction in the accumulated volume error in the spring flood period across all rivers and forecast dates. It is achieved through combinations of different model chains that employ three different approaches to seasonal forecasting into a multi-model ensemble forecast.

The report was prepared by Kean Foster, Cintia Uvo, Jonas Olsson and Johan Södling for the benefit of HUVA - Energiforsk's working group for hydrological development. HUVA incorporates R&D-projects, surveys, education, seminars and standardization. The following are delegates in the HUVA-group:

Peter Calla, Vattenregleringsföretagen (chair.)
Björn Norell, Vattenregleringsföretagen
Stefan Busse, E.ON Vattenkraft
Johan E. Andersson, Fortum
Emma Wikner, Statkraft
Knut Sand, Statkraft
Susanne Nyström, Vattenfall
Mikael Sundby, Vattenfall
Lars Pettersson, Skellefteälvens vattenregleringsföretag
Cristian Andersson, Energiforsk

E.ON Vattenkraft Sverige AB, Fortum Generation AB, Holmen Energi AB, Jämtkraft AB, Karlstads Energi AB, Skellefteå Kraft AB, Sollefteåforsens AB, Statkraft Sverige AB, Umeå Energi AB and Vattenfall Vattenkraft AB partivipates in HUVA.

Stockholm, December 2015

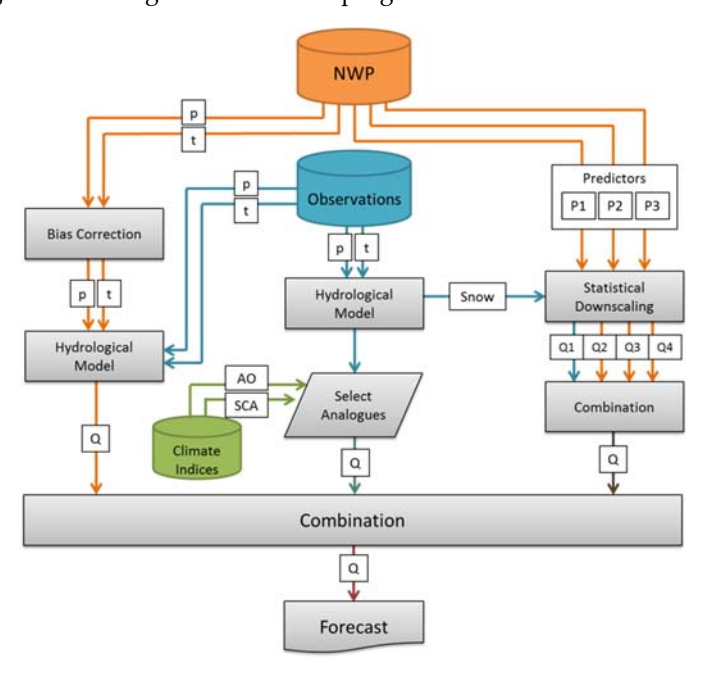
Cristian Andersson

Energiforsk



Sammanfattning

I detta arbete presenterar vi en prototyp av en multimodell för att prognosticera vårflodsvolymen i utvalda vattendrag i norra Sverige. Hydrological Seasonal Forecast System (HSFS) kombinerar olika modellkedjor som använder tre olika metoder för säsongsprognoser för att göra en ensembleprognos med en multimodell.



Med detta nya angreppssätt visar vi att HSFS kan förbättra vårflodsprognosen enligt olika statistiska mått (se tabellen nedan). I medeltal för alla testade älvar och prognosdatum presterar HSFS bättre än de operationella vårflodsprognoserna med IHMS i 62% av fallen och i medeltal med 2% reducerat ackumulerat volymfel för vårflodsprognoserna. Tabellen visar HSFS prestanda för alla älvar och prognostillfällen när MM multi-modellen används för Luleälven, Skellefteälven, Umeälven och Ångermanälven och Δ CMM multi-modellen används för de övriga älvarna.

	IHMS	MM					
	rMAE (%)	rMAE (%)	RI (%)	FY ⁺ (%)			
Jan	22.81	19.77	3.04	61.45			
Feb	22.82	20.01	2.81	62.89			
Mar	22.73	20.88	1.85	59.51			
Apr	22.94	20.58	2.36	58.41			
May	23.98	20.72	3.26	62.47			
Mean	23.06	20.39	2.66	60.95			

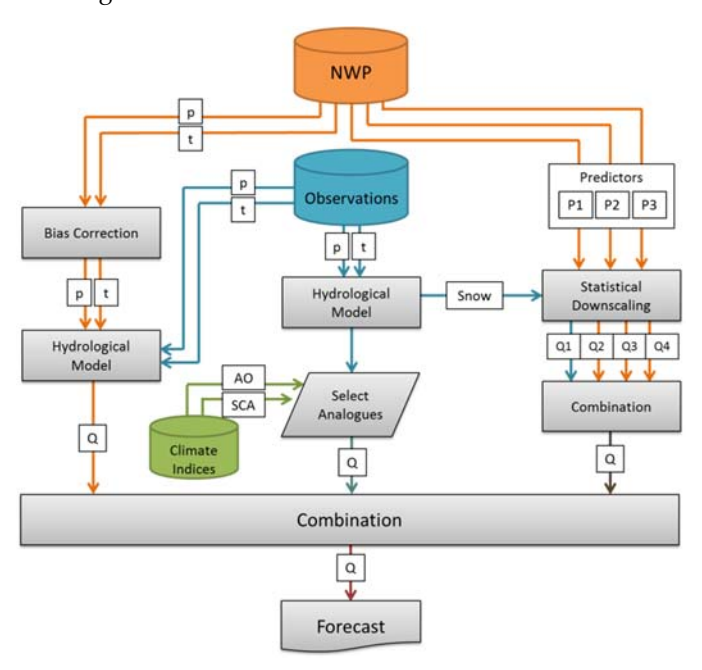


Utvärdering av multimetodmodellen HSFS mot de operationella IHMS-prognoserna för vårflödesvolym vid olika prognostillfällen där rMAE (%) = relative mean absolute error, RI (%) = relative improvement and FY (%) = frequency of years with best performance of the multimethod.



Summary

In this work we present a prototype multi-model system for forecasting the volumes of the spring flood in selected rivers in northern Sweden (a simplified schematic of the model structure can be seen in the image below). The Hydrological Seasonal Forecast System (HSFS) combines different model chains that employ three different approaches to seasonal forecasting into a multi-model ensemble forecast.



With this new approach we show that the HSFS can improve the skill of the spring flood volume forecasts according to different statistical measures. On average the HSFS performs better than the operational IHMS forecasts 62% of the time which translates to a 2% reduction in the accumulated volume error in the spring flood period across all rivers and forecast dates. The table shows the HSFS performance across all rivers and forecast dates when the MM multi-model is used for Luleälven, Skellefteälven, Umeälven and Ångermanälven and the Δ CMM multi-model is used for the remaining rivers.

	IHMS	MM					
	rMAE (%)	rMAE (%)	RI (%)	FY ⁺ (%)			
Jan	22.81	19.77	3.04	61.45			
Feb	22.82	20.01	2.81	62.89			
Mar	22.73	20.88	1.85	59.51			
Apr	22.94	20.58	2.36	58.41			
May	23.98	20.72	3.26	62.47			
Mean	23.06	20.39	2.66	60.95			



Evaluation of the multi method HSFS against the operational IHMS forecasts for spring flood volume at different forecast times according to rMAE (%) = relative mean absolute error, RI (%) = relative improvement and FY (%) = frequency of years with best performance of the multimethod.



List of content

1	Intro	duction		10
2	Mate	erial		11
	2.1	Study	area	11
	2.2	data		14
		2.2.1	Inflow data	14
		2.2.2	Meteorological data	14
		2.2.3	Teleconnection indices (TCI)	16
3	The I	Hydrolog	rical Seasonal Forecast System	17
	3.1	Defini	tion of the spring flood period	17
	3.2	Individ	dual model chains	17
		3.2.1	Analogue ensemble - AE	17
		3.2.2	NWP seasonal forecast ensemble - NE	20
		3.2.3	Statistical downscaling ensemble – SE	20
	3.3	The M	Iulti-model	22
	3.4	Opera	tional aspects	25
4	Expe	rimental	set-up and evaluation protocol	26
5	Evalu	uation Re	esults	28
6	Discu	ussion an	nd Conclusions	31
7	Refe	rences		34
Арр	endix 1			35
App	endix 2			38



1 Introduction

Regulation reservoirs are used by hydropower operators to provide hydraulic head for energy production. They are essential in cold, snow dominated regions where the natural availability of water for energy production is asymmetrically distributed through the year. The purpose of these reservoirs is to save water, and thus energy, from the spring flood period for use during the next winter season. To be able to accommodate the spring flood the lowering of the reservoirs during the winter has to be adapted to the forecasted volume of the spring flood. Reservoir operators use forecasts of inflows to these reservoirs to inform the planning of regulation and production strategies.

The current spring flood forecasting practice in Sweden is a procedure based on the HBV model (e.g. Bergström, 1976; Lindström et al., 1997; Carlsson and Lindström, 2001; Carlsson and Sjögren, 2003). A well calibrated setup of the HBV model is run up to forecast date (typically in February) using observed precipitation and temperatures. This results in a model state that reflects the current hydro-meteorological conditions. Then an ensemble of daily precipitation and temperature observations for the period from the forecast date to the spring flood period are used as input to the HBV model. This results in an ensemble forecast with a climatological evolution through the forecast season from the initial state. This forecast is presented in the form of percentiles.

Olsson et al. (2011) observed that while overall sound and generally useful, this current practice has the obvious limitation that it is based on the climatology, i.e. the normal climate. In their work they investigated alternative methods to forecasting the spring flood. They concluded that some improvements in forecast performance were attainable and that the results warranted further study.

By improving the individual model chains proposed by Olsson et al. (2011), making use of new work by Foster et al. (2015) and employing bias correction to the new system 4 meteorological seasonal forecasts from the ECMWF; it is believed that it is possible to develop a seasonal forecast system for the spring flood period that offers universal improvements in the forecast performance. In this report we present a new Hydrological Seasonal Forecast System (HSFS) prototype aimed at improving the forecasts of the spring flood volumes in Swedish rivers.



2 Material

2.1 STUDY AREA

The HSFS prototype was applied to and evaluated in the following seven hydropower producing river basins Luleälven, Skellefteälven, Umeälven, Ångermanälven, Indalsälven, Ljungan and Ljunsnan (Figure 1). Vindelälven, an unregulated subbasin within the Umeälven system, has been included in this work so as to be able to compare the performance of the HSFS under unregulated conditions.

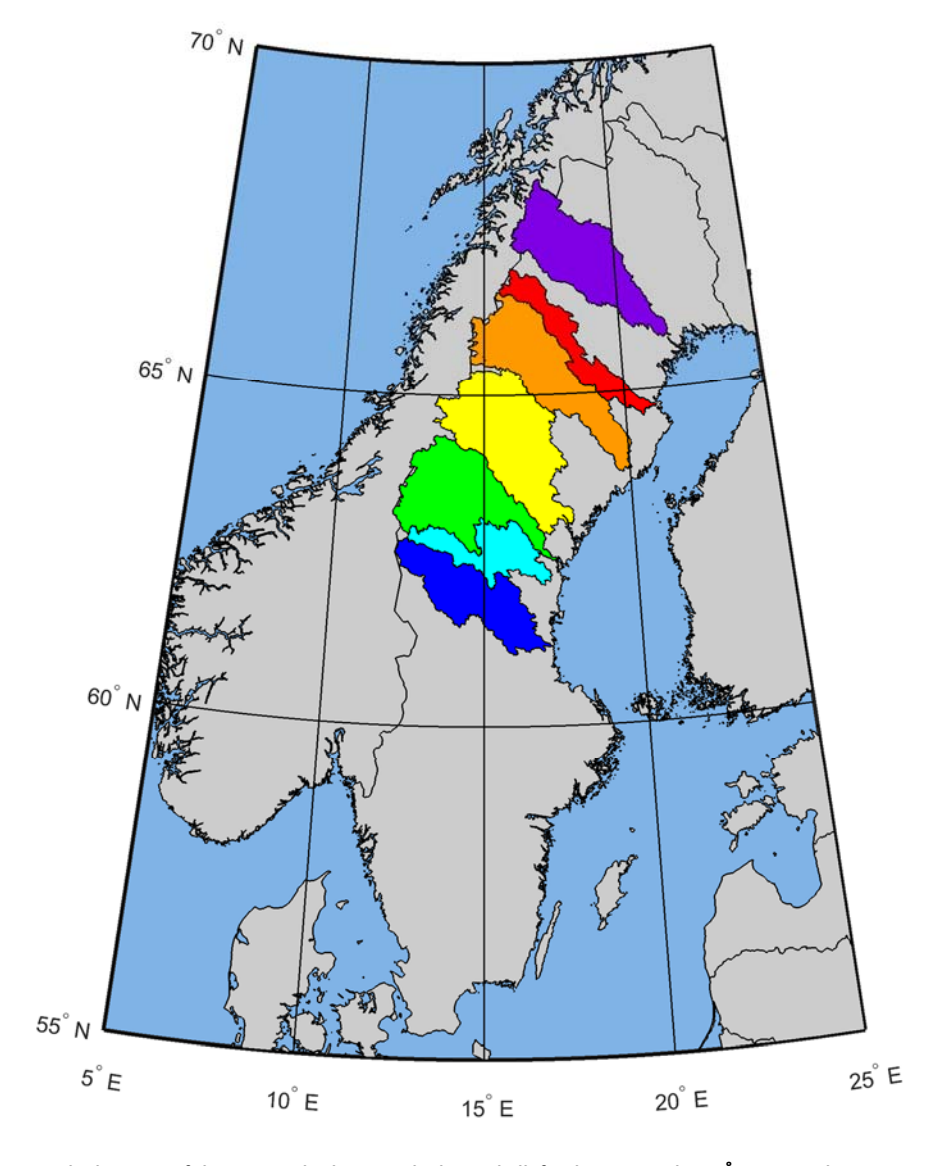


Figure 1. The location of the seven pilot basins Luleälven, Skellefteälven, Umeälven, Ångermanälven, Indalsälven, Ljungan and Ljusnan from north to south respectively.

The gauging stations used in this work correspond to the operational forecast regions defined by SMHI for operational forecasts and three gauging stations along Vindelnälven (Table 1-Table 7). The mean spring flood inflow, Q, given in Table 1, is



calculated as the average spring flood inflow over the period 1981-2015. The overall accuracy in terms of the Nash-Sutcliffe efficiency R² and the relative volume error RVE for the period October 2011 - September 2013 are given in Table 1-Table 7. The hydrological model used in this work is the HBV model (Bergström, 1976; Lindström et al., 1997). On the whole the numbers indicate that the HBV model parameters are well calibrated. The deviation of individual gauging stations from this conclusion can be explained by the quality, or lack thereof, of the observation data for these stations.

Table 1. Basin and station characteristics including performance of the HBV model for Luleälven.

River	Gauging Station	Area	elevation	Mean ΣQ	HBV R ²	RVE (%)
		(km²)	(m)	(m ³ .s ⁻¹)		
Luleälven	Sitasjaure	977	647	9063	0.80	11.8
	Satihaure	1362	699	5965	0.74	4.4
	Suorva	4669	776	34442	0.84	11.3
	Porjus	2890	554	9550	0.80	-9.8
	Messaure	1255	434	4006	0.61	-1.7
	Tjaktjajaure	2256	680	14008	0.85	-7.5
	Parki	2641	600	13441	0.84	-2.7
	Letsi	4681	386	10878	0.70	-13.8
	Boden	4219	155	9283	0.27	10.5

Table 2. Basin and station characteristics including performance of the HBV model for Skellefteälven.

River	Gauging Station	Area	elevation	Mean ΣQ	HBV R ²	RVE (%)
		(km²)	(m)	(m ³ .s ⁻¹)		
Skellefteälven	Sädvajaure	1468	686	9965	0.88	2.6
	Riebnesjaure	976	676	5356	0.67	-9.0
	Hornavan	1767	573	5696	0.70	6.4
	Uddjaur-Storavan	2106	519	4542	0.56	-12.8
	Bergnäs-Vargfors	1372	296	3551	0.29	-2.7
	Vargfors-Rengård	2031	282	4655	0.32	8.1
	Rengård-Kvistfors	1585	135	3067	-1.73	87.6

Table 3. Basin and station characteristics including performance of the HBV model for Umeälven. The gauging stations in italics are in the vindelälven tributary and don't constitute a forecast region.

		.,				
River	Gauging Station	Area	elevation	Mean ΣQ	HBV R ²	RVE (%)
		(km²)	(m)	(m ³ .s ⁻¹)		
Umeälven	Överuman	653	739	5314	0.78	12.3
	Göuta-Ajaure	2538	671	18006	0.93	-2.4
	Abelvattnet	508	664	2950	0.85	-3.5
	Gardiken	728	677	3697	0.53	-31.6
	Storuman	2330	576	6954	0.78	29.7
	Storjuktan	1700	574	6827	0.90	-7.7
	Bålforsen	3169	337	7831	0.56	-8.7
	Harrsele	1827	243	4152	0.44	4.2
	Stornorrfors	13177	212	43297	0.95	-3.2



Table 4. Basin and station characteristics including performance of the HBV model for Ångermanälven.

River	Gauging Station	Area	elevation	Mean ΣQ	HBV R ²	RVE (%)
		(km²)	(m)	(m ³ .s ⁻¹)		
Ångermanälven	Ransaren	610	641	3866	0.90	-0.7
	Kultsjön	1098	629	7207	0.90	3.8
	Malgomaj	1855	515	6630	0.91	-6.7
	Stenkullafors	2392	399	6566	0.82	3.6
	Hällby	2435	330	4181	0.67	3.5
	Lasele	1853	313	3262	0.39	-14.8
	Lövsjön	2383	618	1792	1.00	0.0
	Rörströmssjön	2177	426	6980	0.83	-3.5
	Borgasjön	515	632	3914	0.88	3.4
	Dabbsjön	690	569	3385	0.85	6.5
	Storsjouten	613	577	3775	0.86	-2.0
	Korsselet	331	529	1283	0.33	-16.5
	Tåsjön	773	493	2341	0.66	21.4
	Flåsjön	1058	464	2729	0.60	-4.3
	Lesjön	768	365	1782	0.27	-19.0
	Vängelsjön	567	396	1569	-0.01	24.7
	Kilforsen	829	325	2036	0.36	24.0
	Ankarvattnet	426	598	4262	0.91	-3.5
	Blåsjön	941	591	3507	0.87	2.0
	Jormsjön-Kycklingvattnet	425	594	2637	0.79	-7.1
	Limingen	670	567	5605	0.49	-1.2
	Kvarnbergsvattnet	520	599	2666	0.53	22.4
	Bågede	1497	580	7390	0.87	-11.8
	Ramsele	787	347	1446	0.20	-36.6
	Hjälta	1718	257	2755	0.64	-12.8
	Sollefteå	873	245	1866	-0.01	-36.3

 $\label{thm:continuous} \textbf{Table 5. Basin and station characteristics including performance of the HBV model for Indals\"{a}lven.}$

River	Gauging Station	Area	elevation	Mean ΣQ	HBV R ²	RVE (%)
		(km²)	(m)	(m ³ .s ⁻¹)		
Indalsälven	Torrön	1369	536	9802	0.77	1.1
	Anjan	438	567	2754	0.72	-5.0
	Kallsjön	1212	607	4935	0.59	-15.3
	Östra Noren	2384	599	15571	0.96	-3.7
	Liten	3124	611	1498	0.09	66.5
	Håckren	1166	633	5482	0.91	0.7
	Näkten	493	429	918	0.21	5.8
	Storsjön	4272	482	10777	0.45	-4.5
	Stora Mjölkvattnet	256	590	2316	0.84	-1.9
	Övre Oldsjön	184	612	1692	0.88	-4.4
	Landösjön	1455	552	4164	0.75	1.2
	Rörvattnet	478	584	4380	0.90	-1.2
	Rengen	1110	598	8004	0.90	1.1
	Hotagen	2455	545	3508	0.81	-10.5
	Midskog	2828	449	6672	0.36	10.6
	Gesunden	3808	350	2142	0.19	56.0
	Hammarforsen	3396	328	8781	0.63	10.4
	Oxsjön	233	244	485	0.15	-10.4
	Bergeforsen	1687	216	4197	0.12	-48.6



Table 6. Basin and station characteristics including performance of the HBV model for Ljungan.

River	Gauging Station	Area	elevation	Mean ΣQ	HBV R ²	RVE (%)
		(km²)	(m)	(m ³ .s ⁻¹)		
Ljungan	Storsjön	955	652	4443	0.92	1.2
	Flåsjön	542	628	1689	0.41	-11.2
	Lännässjön	3808	519	3719	0.69	6.3
	Torpshammar	4295	249	6386	0.60	2.2
	Viforsen	1119	207	5119	0.58	-4.7

Table 7. Basin and station characteristics including performance of the HBV model for Ljusnan.

River	Gauging Station	Area	elevation	Mean ΣQ	HBV R ²	RVE (%)
		(km²)	(m)	(m ³ .s ⁻¹)		
Ljusnan	Grundsjön	728	661	3042	0.85	1.7
	Lossen	1357	666	5007	0.89	5.8
	Lofssjön	401	584	1301	0.82	8.6
	Svegsjön	5998	545	15038	0.78	-4.2
	Dönje	6258	183	12012	0.72	-7.1
	Alfta	3130	239	3314	0.65	-1.1

2.2 DATA

2.2.1 Inflow data

Daily inflow data is available since 1981 for the majority of the gauging stations. Missing inflow data was filled by a multiple linear regression approach using simulated inflows for the gauging station and the observations from the surrounding gauging stations as predictors. The average Nash-Sutcliffe efficiency (NSE) for the data used to fill the missing data was 0.82 which indicates that this filling approach is acceptable.

2.2.2 Meteorological data

Historical precipitation and temperature data used in this work were obtained from the PTHBV dataset from SMHI while the meteorological and climate hindcasts used in this work were obtained from the European Centre for Medium-Range Weather Forecasts (ECMWF).

The hindcast data are from the ECMWF system 4 data sets; this numerical weather prediction system (NWP) consists of an ocean analysis to estimate the initial state of the ocean, a global coupled ocean-atmosphere general circulation model to calculate the evolution of the ocean and atmosphere, and a post-processing suite to create forecast products from the raw numerical output.

The ECMWF seasonal forecast system model is the cycle36r4 version of ECMWF IFS (Integrated Forecast System) coupled with a 1° version of the NEMO ocean model. The seasonal forecasts were used in the following two different forms, a field of seasonal averages as input to the statistical model and individual grid points of daily data for input into the HBV model.

The seasonal forecast averages are the seasonal means for each ensemble member of the different predictors which had a domain covering $75^{\circ}W$ to $75^{\circ}E$ and $80^{\circ}N$ to $30^{\circ}N$



(Figure 2) with a 1°x1° resolution. Each predictor has 51 ensemble members for the period 1981-present day. The predictors considered in this part of the work were the following: 850 hPa geopotential, 850 hPa temperature, 850 hPa zonal wind component, 850 hPa meridional wind component, 850 hPa specific humidity, surface sensible heat flux, surface latent heat flux, mean sea level pressure, 10m zonal wind component, 10m meridional wind component, 2m temperature, total precipitation.

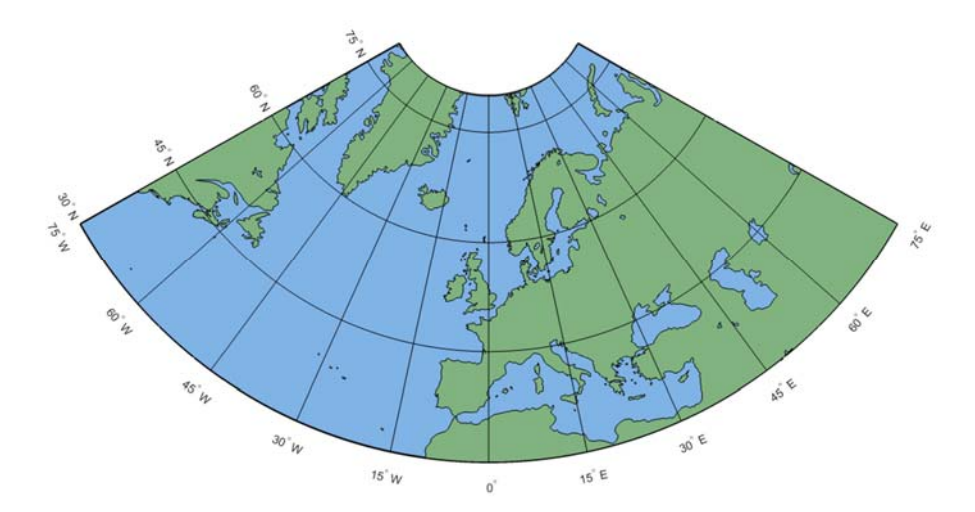


Figure 2. Map showing the Atlantic-European domain of the predictors used in the statistical downscaling model chain.

Daily seasonal forecast - these data are the forecasted daily values of 2 meter temperature and the accumulated total precipitation since the forecast date. These data spanned a period from 1981-2015 and had a domain covering 11°E to 23°E and 55°N to 70°N with a 0.5° x 0.5° resolution. There were 11 ensemble members for each variable for the period 2000-2006 and 41 ensemble members for 1997-2007. Figure 3 shows this 0.5° x 0.5° grid in relation to Sweden.



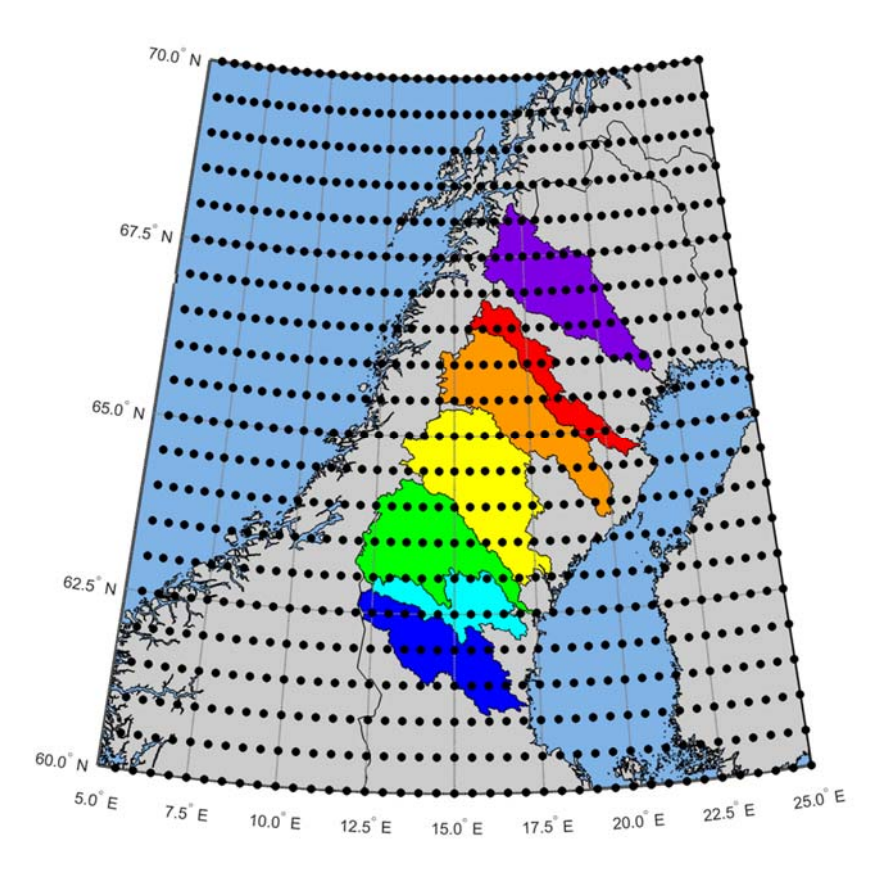


Figure 3. Map showing the ECMWF 0.5°x0.5° grid in relation to the seven river basins in Northern Sweden.

2.2.3 Teleconnection indices (TCI)

The teleconnection patterns (TP) used in this work were the Arctic Oscillation and the Scandinavian Pattern. Indices for these patterns are calculated and made available to the public by the Climate Prediction Center, a part of the National Oceanic and Atmospheric Administration (NOAA).



3 The Hydrological Seasonal Forecast System

3.1 DEFINITION OF THE SPRING FLOOD PERIOD

In previous studies the spring flood period has been defined as the months May-June-July (e.g. Olsson et al., 2011). This definition of the spring flood period is not ideal as it does not take into account the interannual and geographical variations in the timing of the spring flood both within each individual river and between the different rivers. For this work we define the spring flood to be the period from the onset date to the end of July, where the onset is defined as the date after which the inflows are consistently (for a period of time > 30 days) above the 90^{th} percentile of the inflow over the first 80 days of the current year. For forecasts issued in the months after January (February, march, April, and May) the missing inflow data between the 1 January and the forecast date are filled with simulated inflow data from the HBV model using observed precipitation and temperatures as input data.

A drawback to this definition is that the end of the spring flood is not defined according to the hydrograph but rather by date. The reason for not defining the end of the spring flood objectively is twofold. Firstly, the forecast horizon for the ECMWF-SFS is seven months which means that the end of the spring flood in the northern rivers is not always covered by the forecasts made in January, and secondly, a robust and objective definition of what constitutes the end of the spring flood was difficult to achieve within the scope of this work. Further work is needed to accomplish this in any satisfactory manner.

3.2 INDIVIDUAL MODEL CHAINS

Building on initial work by Olsson et al. (2011), three different model chains were employed in this work to improve forecasts of the spring flood volume. In the first chain, an ensemble of analogue input data, selected from historical years, are used as input into the HBV model. In the second chain, bias corrected seasonal climate forecasts of precipitation and temperature, from the ECMWF, are used as input in the HBV model. In the third approach, multivariate statistics are used to downscale seasonal climate forecasts, from ECMWF, and modelled snowpack depth, from HBV, to spring flood volumes.

3.2.1 Analogue ensemble - AE

The large historical meteorological datasets described in section 2.1 are of sufficient length to be a good sample of the natural variability of these variables in the respective locations. Therefore, these data can be considered to be a climatological ensemble where each year is a member. Because of this, it is possible that one or more of the members will be a suitable analogue for the weather during the spring flood period to come.

Two approaches for identifying analogue years were investigated by Olsson et al. (2011). The first was to use teleconnection indices and the second to use circulation pattern analysis as the objective criteria on which to base the selection of analogue years on. However, in this work we have chosen to omit the second approach due to data availability issues under operational conditions (see section3.4).



Teleconnections are defined as persistent and recurring patterns of circulation or air pressure anomalies that affect the climate over a large geographical area and which can have a significant positive or negative correlation with the variability of a geographically separated variable (Panagiotopoulos, 2002). They are identified by a Rotated Principle Component Analysis of standardised geopotential anomalies (Barnston and Livezey, 1987) and indices for a number of the leading northern hemisphere teleconnection patterns are calculated by the Climate Prediction Center at NOAA (National Oceanic and Atmospheric Administration). Foster et al. (2015) investigated the connection between these teleconnection patterns and the spring flood volume in Swedish rivers. They concluded that the three teleconnection patterns most relevant for this study were the North Atlantic Oscillation (NAO), the Arctic Oscillation (AO) and the Scandinavian pattern (SCA). However, due to the large similarities in the spatial patterns and climate impacts of NAO and AO over the Atlantic-European domain (Foster et al., 2015) it was decided to only AO and SCA as the basis for the selection of analogues in this work. The positive phase of the AO is associated with above average temperatures and precipitation over Scandinavia, while the negative phase tends to be associated with below average temperatures and precipitation. The positive phase of the SCA is associated with below average precipitation over Scandinavia.

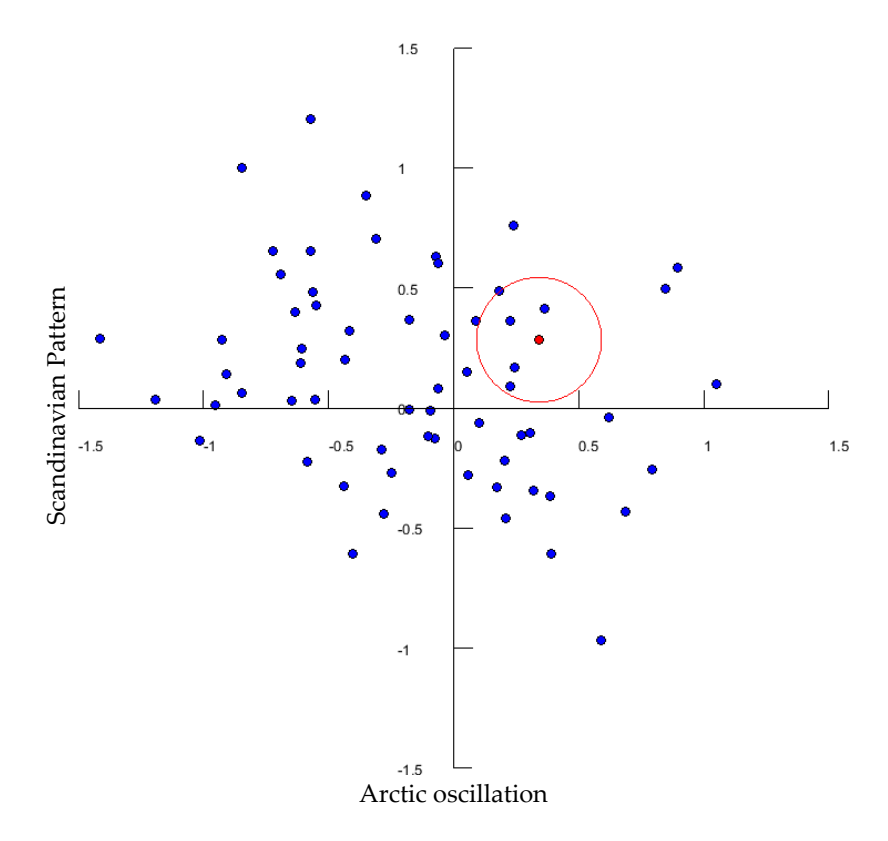


Figure 4. A graphical representation of how an analogue year is selected. The Euclidean space is defined as the plane created when plotting AO indices against SCA indices. The red dot represents the Euclidean position of the forecast year, the red ring is the circle of influence (r = 0.25) and the other dots represent the Euclidean positions of the climatological ensemble for that forecast date. An analogue is defined as all the members of the climatological ensemble that are within this circle of influence.



An improved approach to using these indices for selecting analogues was employed in this work. The mean teleconnection index (TCI) of each pattern is calculated for the period from October to the forecast date minus one month e.g. the period would be October-November-December if the forecast date was in March. This was done for all years in the climatological ensemble. If the values of these indices are considered to be coordinates then their positions can be plotted in Euclidean space. We defined analogue years to be those years whose positions in the resulting AO-SCA Euclidean plane were within a distance of 0.25 from the Euclidean position of the forecast year (Figure 4). The meteorological data for these analogue years are used as input data to the HBV model. If there are no analogue years (there are no historical years with Euclidean positions within the circle of influence) the full climatological ensemble was used as input to the HBV model.

Figure 5 shows the generalized schematic of the AE model chain. Observations of precipitation and temperature are used to run the HBV model up to the forecast date so that the model state is a good approximation of the hydrometeorological conditions. Analogue years are identified using the AO and SCA indices as described above. Then the historical ensemble of precipitation and temperature data are used to run the model to the end of the spring flood period. From these results those ensemble members which correspond to analogue years are selected to form the AE forecast while the rest are discarded.

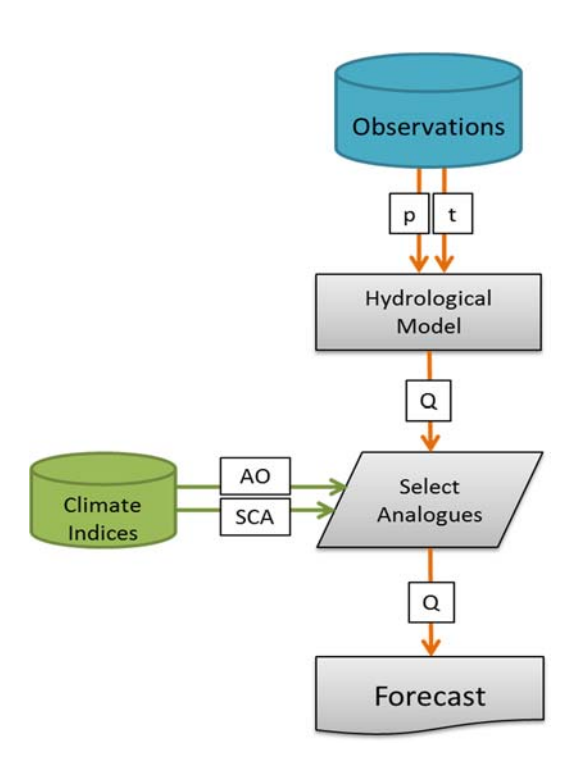


Figure 5. Generalized schematic of the MAE model chain



3.2.2 NWP seasonal forecast ensemble - NE

The NE model chain uses meteorological seasonal forecasts as input data in the HBV model to forecast the spring flood. Figure 6 shows the generalized schematic of the NE model chain. Temperature and precipitation data from the daily ECMWF long-range forecasts are bias corrected against the PTHBV dataset using the DBS methodology (Yang et al., 2010). These bias corrected data were then converted to HBV input files by weighting the grid points according to how much of their areas are within each subbasin. Within the resources of this project, this conversion was only attainable for seven rivers with HBV model set-ups using grid-based input (Luleälven, Skellefteälven, Umeälven, Ångermanälven, Indalsälven, Ljungan and Ljunsnan). These input files are used as input to the HBV model with the same initial state as used in AE model chain.

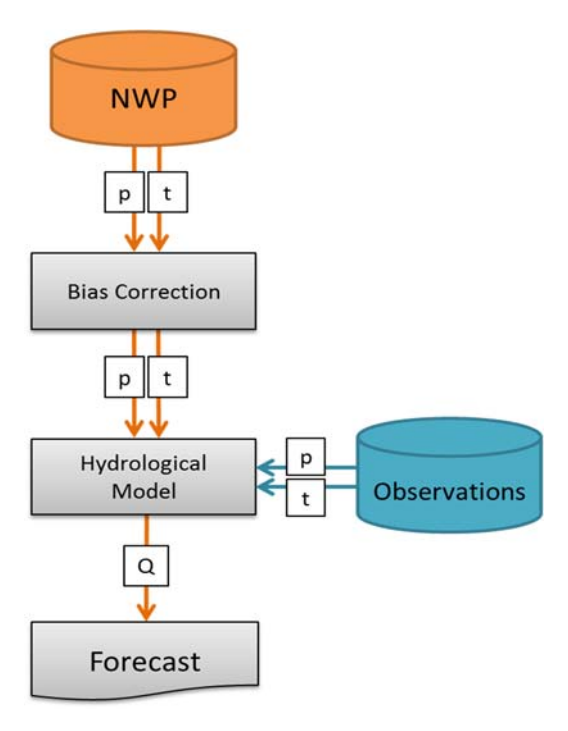


Figure 6. Generalized schematic of the MNE model chain

3.2.3 Statistical downscaling ensemble – SE

Statistical downscaling is a common method used to connect course scaled climate data, typically large scale circulation variables, to finer scaled data, in this case accumulated inflow (e.g. Landman et al., 2001; Foster and Uvo, 2010). The statistical method employed in this work was a singular value decomposition (SVD) analysis. The SVD is a multivariate technique that relates a group of predictors to a group of predictands. SVD is similar to a canonical correlation analysis (CCA) except instead of maximising the temporal correlation between two data fields SVD maximises the temporal covariance between the two fields (Cheng and Dunkerton, 1995).

In this work the predictors were the means of each forecast member of the large scale circulation variable being used. These means were the average for each member of the



monthly means, a derived product available from the ECMWF, for the period from forecast date to the end of July, i.e. if the forecast date were 1 January then the average of each member of the predictor ensemble was calculated for the period 1 January to 31 July. The predictors were chosen by first selecting those which were in agreement with the findings by Foster et al. (2015) and then by performing an analysis on these to select those that explained the most of the variance in the observed spring flood volumes. The predictors used were large scale circulation variables with a 1°x1° resolution from the ECMWF-SFS. The training methodology used was a leave-one-out cross validation approach from 1981-2015. The predictors used in the final forecasts are 850 hPa geopotential, 850 hPa temperature, 850 hPa zonal wind component, 850 hPa meridional wind component, 850 hPa specific humidity, surface sensible heat flux, surface latent heat flux, mean sea level pressure, 10m zonal wind component, 10m meridional wind component, 2m temperature, total precipitation.

Figure 7 shows the generalized schematic of the SE model chain. The three leading variables from the ECMWF-SFS and regional snow data from the HBV initial model state are used as the predictors in the SVD model. The outputted ensembles of spring flood volumes are combined using weights derived from a multivariate linear regression of the outputs and the observed spring flood volumes. The reason that an asymmetric weighting scheme is used here, and not in the multi-model combination (section 3.3), is that there is physical support for it. Early in the season the snowpack, which is the majority contributor to the spring flood volume, is still a fraction of what it will be and is still accumulating. Therefore, the coming meteorological conditions which dictate snowpack evolution are more important early on in the season than later giving physical support for asymmetric weighting.

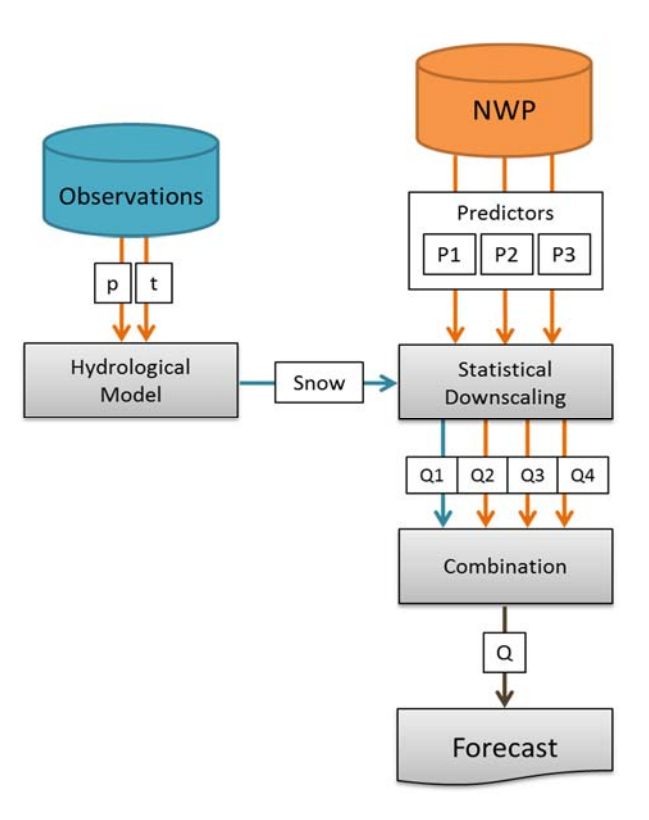


Figure 7. Generalized schematic of the M_{SE} model chain



3.3 THE MULTI-MODEL

The HSFS is a multi-model ensemble of the outputs from the three model chains described above in section 3.2. Figure 8 shows the generalised schematic of the HSFS which combines the three individual model chains into one multi-model system. This combination uses an equal weighting scheme (equation 1). The reason for not using an asymmetric weighting scheme is the lack of data points, 35 in total, from which to derive robust weights from. Attempts to derive weights would risk either:

- 1. Weights that are not based on physical explanations. This can mean a loss of forecast skill by unnecessarily penalising one model over another.
- Over fitting the multi-model system to the calibration period. This means that the multi-model would be biased to the conditions found in calibration period which may reduce forecast skill under other climatic conditions.

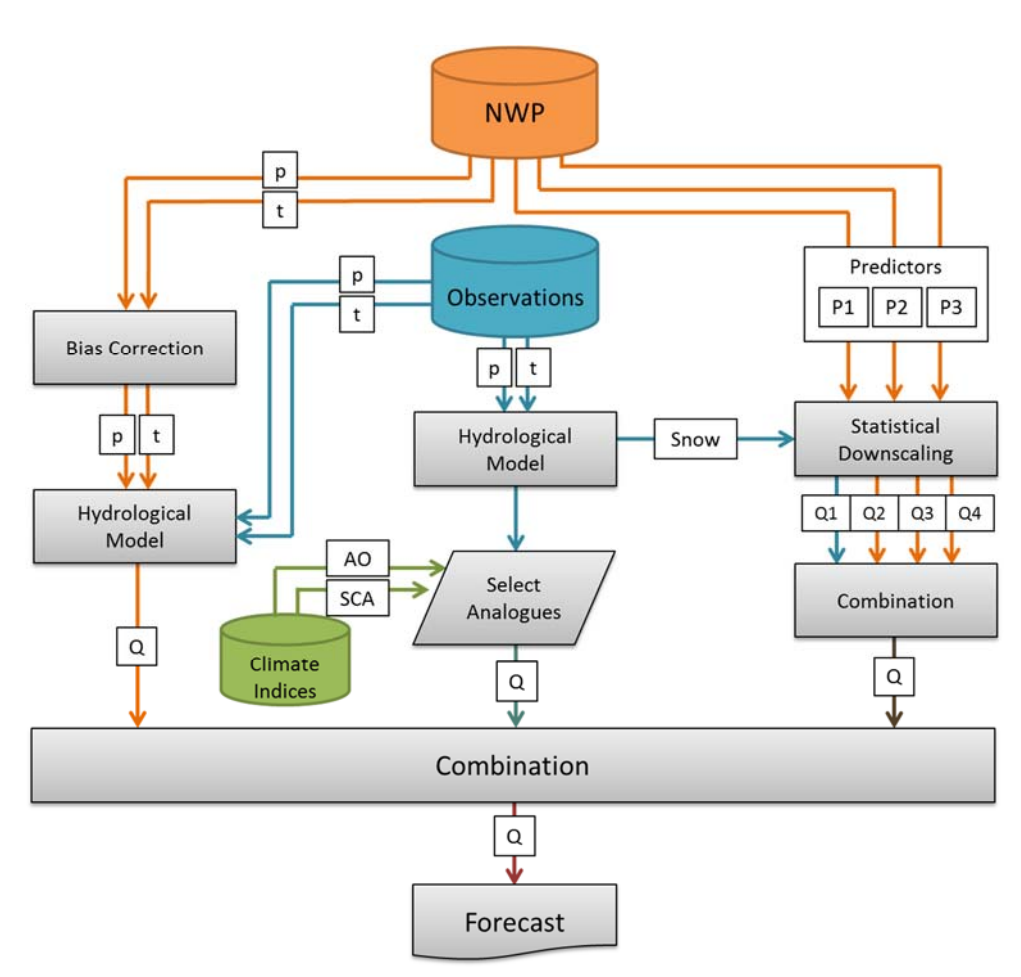


Figure 8. A generalised schematic of the Hydrological Seasonal Forecast System

In their work, Olsson et al. (2011) found that forecast improvement was lower in Ljusnan when compared to Ångermanälven and Vindelälven (a subbasin of Umeälven). They speculated that this was due to the increased influence of precipitation during the spring flood period making it more difficult to forecast. In an effort to improve the multi-model performance, especially in the rivers further south, a



delta change approach was also tested, together with the simple pooling approach, to combat any systematic biases in the model chains.

Simple pooling (MM)

The ensemble sizes of the individual model chains were normalised so that they each had the same number of members to minimise the risk of weighting one model chain over the others. The ensembles from the individual model chains are combined using a simple pooling method according to the following equation:

$$E_{MM_i} = \frac{1}{3} \sum_{i=1}^{n} (E_{AE_i} + E_{NE_i} + E_{SD_i})$$
 (1)

where E_{MM} is the multi-model forecast ensemble, E_{AE} is the analogue forecast ensemble, E_{EH} is the ECMWF driven HBV forecast ensemble, and E_{SD} is the statistical downscaling forecast ensemble.

Delta-change pooling (ΔC MM)

This method is that same as the MM method in the combination of the ensembles into the multi-model ensemble. However, there is a bias correction of the individual model chain forecast ensembles using the delta change approach. The anomalies of the individual ensemble members from the different chains are added to the observed climatology to create new bias corrected ensembles according to the following equation:

$$E_{\Delta CE_i} = \sum_{i=1}^{n} \left((E_i - \overline{E}) + \overline{O} \right) \tag{2}$$

Where $E_{\Delta CE}$ is the bias corrected ensemble, E_i is the individual ensemble member, \overline{E} is the ensemble mean and $\overline{0}$ is the mean of the observed spring flood volumes.

The reason for not applying weights when constructing the multi-model ensemble is due to the lack of data. The length of the data available is too short to be able to make an informed estimate of the individual model weights. It is assumed that with time the amount of data will be sufficient to be able to estimate these weights. Until such a time it is discouraged to use weights due to the risks of overfitting the multi-model to the variability at a specific period in time which could adversely affect its future performance.

Two visualisations are used in the HSFS. The first visualisation presents the ensemble forecast in the form of a boxplot of the multi-model ensemble plotted together with the 33rd and 66th percentiles of historical observed inflows (Figure 9). The percentiles represent thresholds for a below normal (BN), near normal (NN), and above normal (AN) spring flood. The boxplot shows the spread of the ensemble forecast with respect to these thresholds and from this the forecasted probabilities for each category can be calculated.



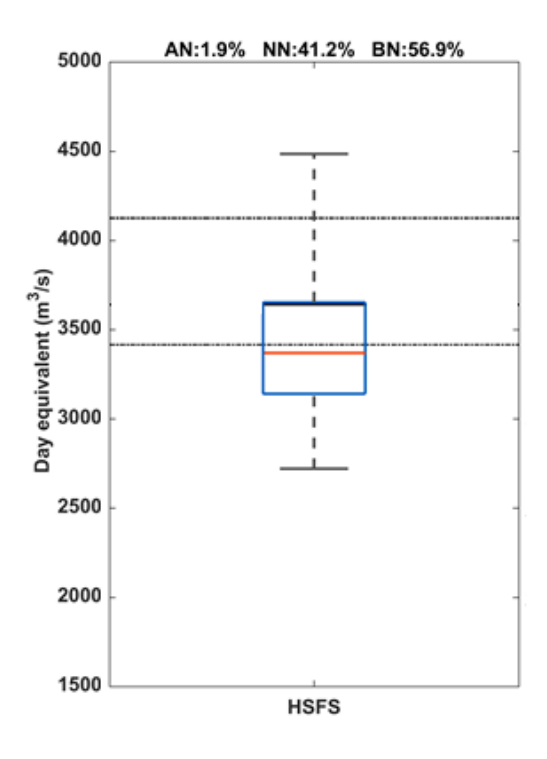


Figure 9. An example forecast using the boxplot visualization method.

The second visualisation presents the ensemble forecast in the form of an OnsetVolume box plotted together with the spaghetti graphs from the AE and NE model chains and the range of historical daily observed inflows (Figure 10). The OnsetVolume box is based on the PeakBox methodology developed by Zappa et al. (2013). It is a visualisation solution that gives the end-user information regarding the probabilistic range of the forecast inflows and spring flood onset. It can be understood as a two dimensional boxplot, one in the horizontal plane giving information on the onset timing, and one in the vertical plane giving information on the spring flood volume. The outer box represents the extreme limits, 0th and 100th percentiles, while the inner box represents the 25th-75th percentile range of the inflow and onset timing. Onset timings are obtained from the AE and NE daily forecast data from which the 0th, 25th, 75th and 100th percentiles calculated. These percentiles determine the boxes coordinates on the x-axis. Similarly, the same percentiles are calculated for the spring flood volume from the multi-model ensemble and these percentiles determine the coordinates of the boxes on the y-axis.



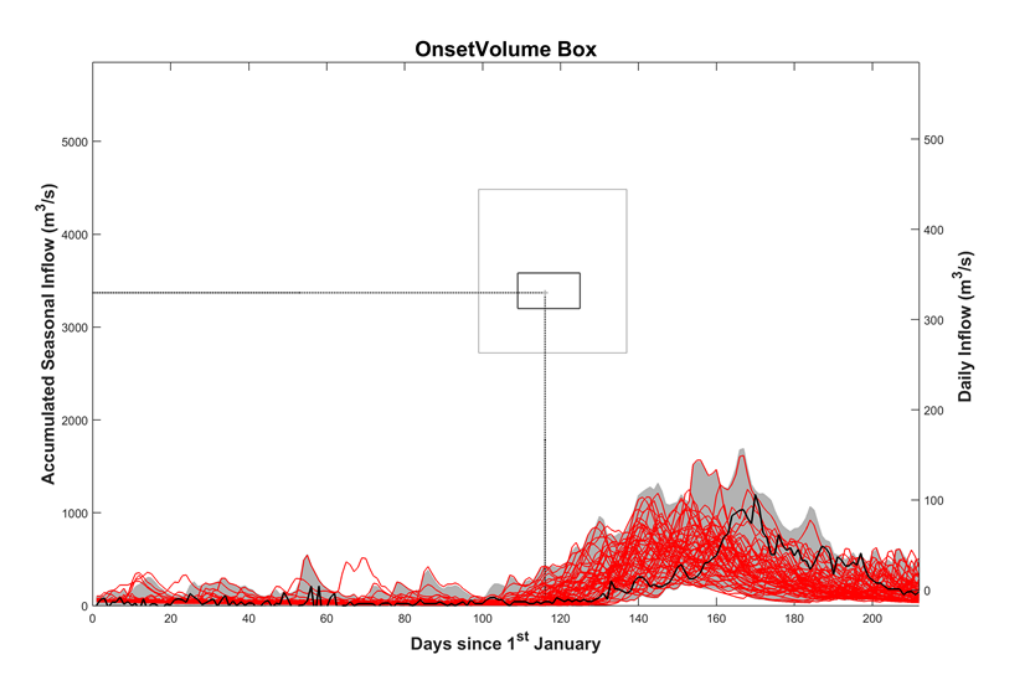


Figure 10. An example forecast using the OnsetVolume box method.

3.4 OPERATIONAL ASPECTS

The most important operational aspect concerns the 'real-time' availability of the meteorological data needed. All three of the model chains are reliant on at least one stream of data that are affected by 'real-time' availability. The AE model chain requires TCI data to select analogues. The CPC publishes updated TCI data on the 1st of every month; however these data have a one month lag thus the HSFS was developed to use lagged TCI data to accommodate this in an operational environment. The NE and SD model chains (sections 3.2.2 and 3.2.3) require meteorological seasonal forecast data from the ECMWF database. These data are updated and made available on the 8th of each month. Thus these approaches may in principle be put into operational use directly.

Another operational aspect concerns the AE forecasts. In the current version of IHMS/HBV it is only possible to select the number of years in the ensemble and not specific years. If the user selects to base the forecast on N years, the most recent N years will be chosen automatically. In this prototype this issue is avoided by selecting the HBV forecasts corresponding to the analogue years from the climatological forecast ensemble. However, it is possible to develop the system to enable the use of N disparate historic years, assuming that a list of the selected years is available. The list could be provided as a text file from the TCI/CP analysis, or it could be entered via the IHMS user interface. Further work would be required to achieve this.



4 Experimental set-up and evaluation protocol

The challenge in this work was to perform a robust evaluation on a limited dataset (34 years) while minimising the risk of unstable or overfitted statistics. Therefore, a leave-one-out cross validation (LOOCV) protocol was adopted. LOOCV is a model evaluation technique that uses n-1 data points to train the models and the data point left out is used for validation. This process is repeated n times to give a validation dataset of length n. This allowed for a robust evaluation with a limited dataset and to be able to sample more of the variability in the training period than if a traditional validation were performed. This is advantageous for evaluating the statistical model which is especially sensitive to situations that were not found within the training period. LOOCV was applied to the individual model chains.

To assess the relative skill for different lead times, we evaluate hindcasts issued on the 8th of January (Jan), 8th of February (Feb), 8th of March (Mar), 8th of April (Apr), and 8th of May (May) for the spring floods 1981-2015. The evaluation of performance is done mainly in terms of how well the accumulated inflow in the spring flood period, Q, is forecasted. This is assessed by rMAE, the relative mean absolute error of a certain forecast (FC), defined as:

$$rMAE = \frac{1}{35} \sum_{y=1981}^{2015} AE^{y}$$
 (3)

where y denotes year and AE^y the absolute error is defined as:

$$AE^{y} = \frac{\left|\sum Q_{\text{obs}}^{y} - \sum Q_{\text{FC}}^{y}\right|}{Q_{\text{obs}}^{y}}$$
(4)

where OBS denotes observation.

To quantify the gain of the two multi-model forecast approaches (section 3.3) their MAE-values are compared with the MAE obtained using the current IHMS procedure by calculating the relative improvement RI (%) according to:

$$RI = rMAE_{IHMS} - rMAE_{FC}$$
 (5)

where IHMS denotes the current operational system and FC denotes the multi-model forecast.

A positive RI indicates that the error of the approach is smaller than the error in the IHMS procedure, and vice versa.



As an additional performance measure, we also calculate the frequency of years in which the new approach performs better than the IHMS procedure, FY+ (%). This may be expressed as:

$$FY^{+} = 100 * \left(\frac{1}{34} \sum_{y=1981}^{2015} H^{y} \right)$$
 (6)

where H is the Heaviside function defined by:

$$H^{y} = \begin{cases} 0, AE_{IHMS}^{y} < AE_{FC}^{y} \\ 1, AE_{IHMS}^{y} > AE_{FC}^{y} \end{cases}$$
 (7)

Relative operating characteristic skill scores (ROCSS) were calculated for the upper ($x \ge 66,7\%$), middle ($66.7\% < x \le 33.3\%$) and lower (x < 33.3%) terciles. These scores estimate the skill of ensemble forecasts to distinguish between below normal (BN), near normal (NN) and above normal (AN) anomalies. Hamill and Juras (2006) define the ROC skill score to be:

$$ROCSS = 2 * AUC - 1 \tag{8}$$

Where AUC is the area under the curve when mapping hit rates against false alarm rates:

$$AUC = \sum_{i=1}^{n+1} \frac{(FAR_i - FAR_{i-1})(HR_i + HR_{i-1})}{2}$$
 (9)

Where FAR = false alarm rate and HR = hit rate. False alarms are defined as both the false positive and false negative forecasts, or type I and type II errors. Hits are defined as correctly forecasted events.



5 Evaluation Results

Table 8 and Table 9 show a summary of the evaluation results by river, this is because the results for the individual stations in each river are in general similar. Complete overviews of the HSFS evaluations are given in Appendices 1 and 2.

Table 8. Summary of MAE, RI and FY⁺ evaluation scores averaged by river. Values for IHMS are in blue, values in black indicate multi-model performance better than IHMS and red values indicatemulti-model performance worse than IHMS.

River	FC Month		MM			ΔC ΜΜ		IHMS
		MAE (%)	RI (%)	FY ⁺ (%)	MAE (%)	RI (%)	FY ⁺ (%)	MAE (%)
Luleälven	Jan	14.96	1.33	62.54	15.17	1.12	58.73	16.29
	Feb	14.58	1.71	65.08	14.86	1.43	60.63	16.29
	Mar	15.49	0.79	60.95	15.69	0.59	60.63	16.28
	Apr	15.01	1.23	62.22	15.29	0.95	57.78	16.24
	May	14.27	1.91	66.35	14.49	1.69	60.95	16.18
Skellefteälven	Jan	18.28	1.21	64.49	19.19	0.30	57.14	19.49
	Feb	18.02	1.48	65.71	19.14	0.36	59.18	19.50
	Mar	19.19	0.31	61.22	19.90	-0.40	55.10	19.50
	Apr	18.28	1.36	61.63	19.05	0.59	57.55	19.64
	May	18.61	1.46	64.49	19.37	0.70	57.55	20.07
Umeälven	Jan	19.16	2.20	63.33	19.42	1.94	57.14	21.36
	Feb	18.48	2.89	69.76	19.18	2.19	60.71	21.37
	Mar	19.44	1.48	61.67	19.77	1.15	57.14	20.92
	Apr	18.15	2.56	60.71	18.47	2.24	56.19	20.71
	May	18.20	2.62	66.90	18.66	2.16	59.29	20.82
Ångermanälven	Jan	20.89	2.01	62.20	21.49	1.41	57.25	22.90
	Feb	20.84	2.06	63.52	21.71	1.19	57.58	22.90
	Mar	21.42	1.37	60.77	21.64	1.15	57.69	22.79
	Apr	20.59	1.93	62.75	21.12	1.40	57.91	22.52
	May	22.05	2.19	66.48	22.17	2.07	57.14	24.24
Indalsälven	Jan	22.89	2.30	61.50	22.53	2.66	58.65	25.19
	Feb	23.05	2.21	63.91	22.88	2.38	58.80	25.26
	Mar	24.75	0.46	60.30	24.28	0.93	58.35	25.21
	Apr	24.24	1.49	59.70	23.68	2.05	59.55	25.73
	May	25.90	1.86	63.76	25.09	2.67	58.95	27.76
Ljungan	Jan	20.33	2.29	64.00	20.36	2.26	59.43	22.62
	Feb	21.73	0.89	62.29	22.07	0.55	58.29	22.62
	Mar	23.30	-0.70	56.00	23.23	-0.63	53.14	22.60
	Apr	23.57	-0.77	51.43	23.87	-1.07	52.00	22.80
	May	23.62	0.75	56.00	23.59	0.78	53.14	24.37
Ljusnan	Jan	28.46	3.33	63.81	22.19	9.60	59.52	31.79
	Feb	28.81	3.00	63.33	23.21	8.60	59.05	31.81
	Mar	29.17	2.63	60.00	23.11	8.69	60.48	31.80
	Apr	29.90	3.07	54.76	24.51	8.46	50.00	32.97
	May	30.61	3.80	61.90	23.24	11.17	60.95	34.41
Average		21.32	1.98	62.13	20.67	2.90	57.95	23.06



The MAE values for the MM, Δ CMM and IHMS show a general north south gradient in the performance of spring flood forecasts with relative MAE values in ranging from the mid-teens in the north to the mid-thirties in the south. This can be explained by the increasing influence of precipitation, a large source of uncertainty in the forecasts, to the spring flood the further south you go.

We expected a general improvement in performance values as the forecast date approaches the spring flood period and although the data supports this the improvements were much lower than anticipated. We think that this is a result of using the onset date to define the beginning of the spring flood instead of a fixed date. We see the use of the onset date as a more descriptive approach and thus superior to the fixed date approach. As the onset was defined globally there may be scope for some improvement by 'calibrating' the definition for each river (and even gauging station) individually. It should be noted that there is typically a drop in performance in the May forecasts in most of the rivers and even in the April forecasts in the southern rivers. This can be explained by the spring flood having already started prior to the forecast date in many cases.

Both the MM and the Δ CMM outperform IHMS when looking at the performance values in Table 8. The only exception is the April forecasts in Ljugan. In the northernmost rivers the MM outperforms the Δ CMM while this is reversed for the southernmost rivers save for FY $^+$ where MM is consistently better.

The ROCSS in Table 9 show that the two multi-models generally have better skill than IHMS in predicting the anomalous years. This is seen in the larger ROCSS values for the BN and AN forecasts. However, IHMS is more skilful in predicting near normal spring floods. This result is expected as IHMS forecasts are climatological in nature and should therefore do well in near normal years. Again, MM generally shows better performances than Δ CMM with the MM having ROCSS on average 0.03 better than Δ CMM.

Individual values for stations can differ markedly (see appendices 1 and 2) from the values reported in this section. It can be noted that these deviations typically occur for stations where the NSE values in Table 1-Table 7 are low. This indicates that when the HBV model is not well calibrated and that the observed inflows are excessively noisy then the HSFS performance drops. The reason for this is that it is difficult to calibrate the statistical model properly when the observations fluctuate too much due to noise; the method breaks down because the noise obscures the predictive signal. The AE and NE model chains are directly affected by the poorly performing model as well as the uncertainty in the observations.



Table 9. Average ROC skill scores per river. Values for IHMS are in blue, values in black indicate multi-model performance better than IHMS and red values indicatemulti-model performance worse than IHMS.

River	FC Month		MM			ΔC ΜΜ			IHMS	
		BN	NN	AN	BN	NN	AN	BN	NN	AN
Luleälven	Jan	0.39	0.04	0.29	0.34	0.07	0.26	0.21	0.10	0.09
	Feb	0.44	0.09	0.24	0.40	0.14	0.19	0.22	0.11	0.09
	Mar	0.39	0.09	0.12	0.34	0.12	0.08	0.21	0.11	0.09
	Apr	0.38	-0.02	0.20	0.35	-0.02	0.19	0.21	0.12	0.09
	May	0.44	0.08	0.39	0.40	0.09	0.37	0.25	0.10	0.08
Skellefteälven	Jan	0.35	-0.03	0.14	0.33	-0.06	0.12	0.25	0.13	-0.01
	Feb	0.44	0.04	0.12	0.40	0.00	0.12	0.26	0.13	-0.01
	Mar	0.39	-0.04	-0.06	0.35	-0.10	-0.06	0.26	0.14	0.00
	Apr	0.37	0.01	0.02	0.33	-0.05	0.01	0.26	0.13	-0.01
	May	0.36	-0.01	0.12	0.30	-0.07	0.10	0.20	0.09	0.00
Umeälven	Jan	0.32	-0.02	0.17	0.32	0.02	0.15	0.22	0.18	0.02
	Feb	0.43	0.13	0.23	0.41	0.08	0.21	0.22	0.19	0.04
	Mar	0.31	0.04	0.10	0.26	-0.04	0.05	0.21	0.17	0.03
	Apr	0.43	0.04	0.23	0.35	-0.02	0.23	0.21	0.16	0.03
	May	0.49	0.02	0.30	0.41	-0.04	0.31	0.22	0.09	0.09
Ångermanälven	Jan	0.40	0.14	0.18	0.34	0.11	0.15	0.30	0.14	0.18
	Feb	0.45	0.15	0.25	0.40	0.05	0.25	0.30	0.14	0.18
	Mar	0.37	0.08	0.19	0.31	0.07	0.18	0.29	0.13	0.18
	Apr	0.44	0.16	0.30	0.37	0.12	0.28	0.29	0.12	0.18
	May	0.44	0.11	0.31	0.39	0.07	0.30	0.22	0.15	0.09
Indalsälven	Jan	0.38	0.15	0.24	0.32	0.07	0.16	0.21	0.07	0.18
	Feb	0.40	0.16	0.35	0.32	0.05	0.33	0.21	0.07	0.18
	Mar	0.24	0.07	0.14	0.19	0.09	0.08	0.22	0.09	0.19
	Apr	0.31	0.07	0.18	0.26	0.06	0.15	0.22	0.07	0.18
	May	0.23	-0.10	0.26	0.18	-0.12	0.23	0.18	0.03	0.10
Ljungan	Jan	0.59	0.05	0.26	0.58	0.04	0.18	0.38	0.03	0.32
	Feb	0.42	0.02	0.39	0.39	-0.11	0.38	0.38	0.03	0.32
	Mar	0.27	-0.07	0.17	0.18	-0.19	0.13	0.39	0.03	0.32
	Apr	0.24	-0.09	0.09	0.24	-0.13	0.02	0.37	0.06	0.27
	May	0.29	-0.21	0.38	0.26	-0.26	0.31	0.26	-0.01	0.12
Ljusnan	Jan	0.41	0.02	0.38	0.42	0.01	0.33	0.33	0.05	0.32
	Feb	0.33	-0.05	0.47	0.28	-0.02	0.45	0.32	0.05	0.32
	Mar	0.22	-0.07	0.26	0.24	-0.05	0.14	0.33	0.05	0.32
	Apr	0.17	0.02	0.19	0.19	0.09	0.15	0.33	0.11	0.31
	May	0.19	0.01	0.31	0.19	-0.02	0.25	0.16	0.13	0.22
Average		0.36	0.03	0.23	0.32	0.00	0.19	0.26	0.10	0.15



6 Discussion and Conclusions

Both multi-model approaches generated showed general improvements for all rivers with the largest gains being attainable for Ljusnan. This is probably because the spring floods in this river it is mixed with rain and therefore more difficult to forecast whereas the multi-models ensembles include the SD approach which is not affected by uncertainties in precipitation to the same extent as the other model chains. However, both the MM and Δ CMM showed mixed results for Ljungan. The hypothesised explanation for this is threefold:

- The HBV model does not simulate the hydrology in this river as well as in other rivers (see Table 6).
- The observed inflows at a number of stations within the Ljungan system are noisy, the values fluctuate greatly in a short time frame, which both makes it difficult calibrate the statistical model and increases the uncertainty in the observations.
- The increased influence of rain on snow processes leading into the spring flood in Ljungan means that any uncertainty in the precipitation data used in the different model chains would be more noticeable in the forecasts than in the rivers further north.

On average the HSFS performs better than IHMS 62% of the time which translates to a 2% reduction in volume error across all rivers and forecast dates. The MM combination approach is generally preferred to the Δ CMM approach; however larger reductions in forecast errors are attainable with the latter in the southernmost rivers. This means that depending on the goals of the end-user it may be beneficial to use a setup that uses the MM approach for Luleälven, Skellefteälven, Umeälven, and Ångermanälven and the Δ CMM approach for Indalsälven, Ljungan and Ljusnan.

The performance of the HSFS would be enhanced further if a weighting scheme were employed to the combination of the individual model chains. However, due to the limited data lengths available it is not possible to implement such a system without the risk of overfitting the resulting multi-model to the calibration period. With time the amount of data will make it possible to employ weighting. Additionally, further improvements in the quality of meteorological seasonal forecasts are expected which would enhance the HSFS performance.

At present the predictors used in the statistical model chain are selected regionally and not locally or for each station individually. Some improvement in model performance may be achievable if predictors were selected more locally. But caution should be exercised here too as the use of fewer predictands in the selection process increases the risk for predictors to be identified erroneously. The statistical analysis becomes unstable when the sample sizes are too small.

There is scope for future studies to improve the performance of the HSFS. These can be divided into two groups, technical related and interface related. As mentioned previously the spring onset has a global definition and it is not entirely incorrect to assume that a more local calibration of this definition would result in better performances. Other technical work would be to investigate the added value of increasing the number of model chains in the HSFS. By including alternative input data



streams and hydrological models could improve the HSFS' sampling of the uncertainty and in turn improve the quality and robustness of the seasonal forecast.

More work is needed to develop visualisation approaches that better communicate the information to the end-user which will ultimately make the forecasts more actionable. It is important that this work be done together with the end-users. Also, this should be combined with developing ways to train end-users on how to make better use of probabilistic forecasts.



7 Acknowledgements

The authors would like to thank Peter Berg and Thomas Bosschard for their help with bias correction calculations, Jonas German and Gitte Berglöv for their help in implementing the HBV model into the HSFS and Wei Yang for fruitful discussions regarding analogue year selection.

This work benefitted from funding additional from the FORMAS project HYDROIMPACTS 2.0 (project number 2009-525) and the European FP7 project EUPORIAS (Grant Agreement 308291).



8 References

- Barnston, G., Livezey, R.E (1987) Classification, seasonality and lowfrequency atmospheric circulation patterns, Monthly Weather Review 115:1083-1126.
- Bergström, S., (1976) Development and application of a conceptual runoff model for Scandinavian catchments, SMHI Reports RHO, No. 7, Norrköping.
- Carlsson, B., Lindström, G. (2001) HBV-modellen och flödesprognoser, SMHI Reports Hydrology No. 85 (in Swedish).
- Carlsson, B., Sjögren, J. (2003) Uppdatering och hydrologiska långtidsprognoser en jämförelse mellan olika metoder, Report No. 43, SMHI, Norrköping (in Swedish).
- Cheng, X., Dunkerton, T.J. (1995) Orthogonal rotation of spatial patterns derived from singular value decomposition analysis, Journal of Climate 8:2631-2643.
- Foster, K.L., Uvo, C.B. (2010) Seasonal streamflow forecast: a GCM multimodel downscaling approach, Hydrology Research 41:503-507.
- Foster, K., Uvo, C.B., and J. Olsson (2015) The spatial and temporal effect of selected teleconnection phenomena on Swedish hydrology. *Manuscript in preparation*.
- Hamill, T. M., & Juras, J. (2006). Measuring forecast skill: is it real skill or is it the varying climatology?. Quarterly Journal of the Royal Meteorological Society, 132(621C), 2905-2923.
- Landman, W.A., Mason, S.J., Tyson, P.D., Tennant, W.J. (2001) Statistical downscaling of GCM simulations to Streamflow, Journal of Hydrology 252:221-236.
- Lindström, G., Johansson, B., Persson, M., Gardelin, M., Bergström, S., (1997)

 Development and test of the distributed HBV-96 hydrological model, Journal of Hydrology 201:272–288.
- Zappa, M., Fundel, F., & Jaun, S. (2013). A 'Peak-Box'approach for supporting interpretation and verification of operational ensemble peak-flow forecasts. Hydrological Processes, 27(1), 117-131.
- Olsson, J., Uvo, C.B., Foster, K., Yang, W., Södling, J., German, J., and B. Johansson (2011) A multi-model system for spring flood forecasts, Elforsk Rapport 11:72, The Swedish Electrical Utilities R&D Company, Stockholm, 29 pp.
- Panagiotopoulos, F., Shahgedanova, M., and Stephenson, D. B. (2002, November). A review of Northern Hemisphere winter-time teleconnection patterns. In Journal de Physique IV (Proceedings) (Vol. 12, No. 10, pp. 27-47). EDP sciences.
- Yang, W., Andr'easson, J., Graham, L. P., Olsson, J., Rosberg, J., and Wetterhall, F.: Distribution-based scaling to improve usability of regional climate model projections for hydrological climate change impacts studies, Hydrol. Res., 41, 211–229, 2010.



Appendix 1

RI and FY⁺ results for the MM version of the HSFS per station for each river.

		Já	an	Fe	eb	M	ar	Α	pr	М	ay
River	Gauging Station	RI	$FY^{^+}$	RI	FY^{+}	RI	FY^{+}	RI	FY^{+}	RI	$FY^{^+}$
Luleälven	Sitasjaure	1.1	60.0	1.0	62.9	1.3	62.9	1.4	57.1	1.5	65.7
	Satihaure	2.4	65.7	3.3	71.4	1.2	57.1	2.1	68.6	2.7	77.1
	Suorva	1.1	65.7	1.5	65.7	1.6	60.0	2.4	62.9	2.9	71.4
	Porjus	2.1	62.9	2.0	71.4	1.4	68.6	1.2	65.7	1.8	68.6
	Messaure	0.9	57.1	2.2	62.9	0.7	62.9	2.8	68.6	1.5	65.7
	Tjaktjajaure	2.1	65.7	1.8	68.6	1.1	62.9	0.8	57.1	1.9	65.7
	Parki	1.4	68.6	1.6	65.7	0.4	60.0	0.5	60.0	1.8	60.0
	Letsi	0.8	62.9	0.8	62.9	-0.0	60.0	0.8	62.9	1.1	51.4
	Boden	-0.1	54.3	1.2	54.3	-0.6	54.3	-1.0	57.1	1.9	71.4

		Ja	an	Fe	eb	M	lar	Α	pr	М	ay
River	Gauging Station	RI	FY⁺	RI	$FY^{^{+}}$	RI	FY^{+}	RI	FY⁺	RI	FY ⁺
Skellefteälven	Sädvajaure	0.9	71.4	1.9	62.9	0.8	65.7	1.6	60.0	2.2	68.6
	Riebnesjaure	1.1	60.0	2.4	77.1	0.7	65.7	1.4	62.9	2.1	71.4
	Hornavan	1.4	65.7	2.5	62.9	0.4	65.7	0.9	60.0	1.7	60.0
	Uddjaur-Storavan	1.2	68.6	0.3	60.0	0.7	62.9	1.3	62.9	0.8	65.7
	Bergnäs-Vargfors	1.5	65.7	1.6	65.7	0.6	57.1	1.8	62.9	0.4	65.7
	Vargfors-Rengård	0.3	60.0	0.1	65.7	-0.2	57.1	0.3	60.0	1.7	62.9
	Rengård-Kvistfors	2.1	60.0	1.5	65.7	-0.8	54.3	2.2	62.9	1.4	57.1

		Ja	an	Fe	eb	М	ar	Α	pr	М	ay
River	Gauging Station	RI	FY ⁺	RI	FY⁺	RI	$FY^{^+}$	RI	FY^{+}	RI	$FY^{^{+}}$
Umeälven	Överuman	-0.8	45.7	0.9	60.0	-0.8	54.3	1.9	60.0	1.9	62.9
	Göuta-Ajaure	1.4	65.7	3.4	80.0	2.5	62.9	3.5	74.3	3.6	77.1
	Abelvattnet	0.5	68.6	2.4	77.1	2.0	65.7	3.5	68.6	3.8	71.4
	Gardiken	8.6	80.0	10.4	82.9	5.2	74.3	3.6	71.4	3.1	68.6
	Storuman	1.3	60.0	-0.1	62.9	-0.1	57.1	-0.2	40.0	1.1	57.1
	Storjuktan	1.0	65.7	1.5	74.3	0.2	60.0	1.3	51.4	1.3	65.7
	Bålforsen	0.9	57.1	0.3	57.1	-0.2	51.4	1.1	48.6	0.1	62.9
	Harrsele	0.4	51.4	2.0	62.9	0.9	62.9	2.1	65.7	1.9	60.0
	Laisvall	7.4	71.4	6.2	74.3	4.1	62.9	8.0	71.4	8.1	74.3
	Sorsele	1.5	65.7	2.9	68.6	1.7	71.4	2.4	60.0	3.1	74.3
	Vindeln	2.3	65.7	2.5	65.7	1.2	57.1	1.7	57.1	1.8	62.9
	Stornorrfors	1.8	62.9	2.5	71.4	1.0	60.0	1.7	60.0	1.7	65.7



		Ja	an	Fe	eb	М	ar	Α	pr	М	ay
River	Gauging Station	RI	FY^{+}	RI	$FY^{^{+}}$	RI	$FY^{^{+}}$	RI	FY^{+}	RI	$FY^{^{+}}$
Ångermanälven	Ransaren	4.8	82.9	5.7	85.7	4.4	77.1	2.7	60.0	3.8	74.3
	Kultsjön	3.5	77.1	4.9	80.0	3.1	71.4	2.3	54.3	3.4	77.1
	Malgomaj	2.6	65.7	2.2	68.6	0.9	60.0	0.7	60.0	1.0	57.1
	Stenkullafors	2.2	65.7	1.1	65.7	0.2	57.1	-0.4	57.1	1.9	71.4
	Hällby	1.3	57.1	5.9	60.0	4.9	54.3	4.6	57.1	4.4	60.0
	Lasele	-0.9	42.9	-1.9	51.4	-0.7	51.4	-0.8	51.4	-0.8	45.7
	Lövön	1.5	54.3	1.0	60.0	0.7	57.1	2.3	68.6	2.9	80.0
	Rörströmssjön	1.6	62.9	3.6	68.6	2.7	62.9	4.0	71.4	3.5	68.6
	Borgasjön	2.3	62.9	3.2	68.6	2.0	74.3	2.2	68.6	3.7	80.0
	Dabbsjön	0.4	57.1	1.0	57.1	0.6	62.9	2.4	62.9	1.7	57.1
	Storsjouten	2.0	60.0	1.4	62.9	0.4	54.3	1.9	65.7	1.8	62.9
	Korsselet	3.1	60.0	3.2	65.7	1.6	54.3	2.9	62.9	2.1	62.9
	Tåsjön	4.6	74.3	1.9	65.7	1.0	57.1	2.8	74.3	1.5	62.9
	Flåsjön	-1.7	54.3	-1.5	62.9	-1.1	57.1	0.0	54.3	4.3	82.9
	Lesjön	0.3	51.4	0.5	54.3	-1.0	42.9	1.2	57.1	0.5	65.7
	Vängelsjön	0.1	65.7	0.1	51.4	-0.2	54.3	-0.0	54.3	0.8	62.9
	Kilforsen	2.9	60.0	3.3	65.7	2.6	68.6	2.5	62.9	0.2	54.3
	Ankarvattnet	1.5	68.6	3.0	62.9	2.8	62.9	4.5	71.4	3.3	77.1
	Blåsjön	5.2	68.6	7.2	77.1	5.1	71.4	6.3	80.0	3.6	80.0
	Jormsjön-Kycklingvattnet	5.4	74.3	5.2	74.3	5.7	80.0	4.5	71.4	2.2	68.6
	Limingen	2.0	65.7	4.0	62.9	3.0	68.6	4.2	74.3	2.7	62.9
	Kvarnbergsvattnet	5.7	77.1	4.2	68.6	3.8	71.4	4.3	77.1	3.2	77.1
	Bågede	2.7	57.1	0.7	57.1	-0.2	51.4	2.1	60.0	2.0	62.9
	Ramsele	4.9	54.3	1.3	54.3	-0.1	45.7	0.8	54.3	8.0	74.3
	Hjälta	-0.1	51.4	-3.4	42.9	-2.6	54.3	-4.0	48.6	-1.1	57.1
	Sollefteå	-5.5	45.7	-4.4	57.1	-3.9	57.1	-3.9	51.4	-3.7	42.9

		Ja	ın	Fe	eb	М	ar	A	pr	М	ay
River	Gauging Station	RI	FY^{+}	RI	$FY^{^+}$	RI	FY^{+}	RI	FY^{+}	RI	FY^{+}
Indalsälven	Torrön	0.1	54.3	2.7	62.9	1.3	62.9	3.5	77.1	2.1	62.9
	Anjan	2.0	62.9	3.4	62.9	0.1	60.0	2.3	65.7	1.5	60.0
	Kallsjön	-1.7	51.4	0.0	54.3	-0.7	54.3	1.6	60.0	1.8	65.7
	Östra Noren	5.2	74.3	4.9	68.6	3.1	65.7	2.0	57.1	1.8	60.0
	Liten	7.8	68.6	6.7	65.7	4.5	65.7	9.2	60.0	14.5	77.1
	Håckren	3.1	68.6	3.9	74.3	1.2	68.6	0.5	57.1	1.1	60.0
	Näkten	0.5	62.9	1.0	48.6	-2.0	48.6	-3.1	37.1	-2.7	51.4
	Storsjön	2.3	68.6	-0.2	60.0	-3.0	45.7	-1.9	57.1	-2.8	51.4
	Stora Mjölkvattnet	2.1	60.0	3.4	71.4	2.1	62.9	3.2	80.0	3.1	68.6
	Övre Oldsjön	1.7	54.3	2.3	65.7	1.9	65.7	1.6	68.6	2.3	60.0
	Landösjön	1.1	54.3	1.2	62.9	0.4	54.3	1.5	60.0	2.5	68.6
	Rörvattnet	3.8	62.9	3.7	74.3	2.7	77.1	1.3	60.0	2.6	65.7
	Rengen	2.5	62.9	2.9	68.6	2.4	65.7	2.6	68.6	2.7	71.4
	Hotagen	7.3	77.1	5.4	74.3	3.6	68.6	3.7	62.9	4.2	71.4
	Midskog	1.5	57.1	1.7	60.0	-0.1	45.7	1.1	45.7	-0.4	51.4
	Gesunden	3.5	57.1	-0.8	54.3	-8.5	42.9	1.1	57.1	4.4	71.4
	Hammarforsen	1.5	57.1	0.9	60.0	1.3	65.7	2.4	54.3	3.7	68.6
	Oxsjön	-2.5	45.7	-2.1	54.3	-3.6	54.3	-2.4	54.3	-1.6	62.9
	Bergeforsen	1.8	68.6	0.8	71.4	2.1	71.4	-2.0	51.4	-5.5	62.9



		Ja	an	Fe	eb	М	ar	Α	pr	M	ay
River	Gauging Station	RI	FY^{+}	RI	$FY^{^{+}}$	RI	FY^{+}	RI	FY^{+}	RI	$FY^{^{+}}$
Ljungan	Storsjön	2.2	65.7	2.6	65.7	1.1	57.1	1.4	62.9	2.2	62.9
	Flåsjön	4.6	71.4	3.5	74.3	2.4	71.4	2.3	65.7	1.4	57.1
	Lännässjön	2.6	60.0	0.5	54.3	-1.2	48.6	-1.2	45.7	-0.0	48.6
	Torpshammar	1.2	62.9	0.2	57.1	-2.2	45.7	-2.6	48.6	-0.7	54.3
	Viforsen	0.8	60.0	-2.4	60.0	-3.6	57.1	-3.7	34.3	0.8	57.1

		Jä	an	Fe	eb	М	ar	Α	pr	M	ay
River	Gauging Station	RI	FY [⁺]	RI	FY [⁺]	RI	FY [⁺]	RI	FY [⁺]	RI	$FY^{^{+}}$
Ljusnan	Grundsjön	2.1	62.9	1.5	60.0	0.6	62.9	0.7	57.1	1.3	54.3
	Lossen	2.3	65.7	2.3	68.6	0.5	54.3	1.1	62.9	2.6	57.1
	Lofssjön	0.5	57.1	1.2	57.1	-0.1	57.1	-0.8	40.0	4.5	68.6
	Svegsjön	2.1	65.7	1.9	60.0	0.6	54.3	-1.5	51.4	2.0	68.6
	Dönje	1.3	60.0	1.7	62.9	1.1	60.0	-3.7	31.4	-0.5	45.7
	Alfta	11.6	71.4	9.4	71.4	13.1	71.4	22.6	85.7	12.9	77.1



Appendix 2

RI and FY+ results for the ΔCMM version of the HSFS per station for each river.

		Já	an	Fe	eb	M	lar	Α	pr	М	ay
River	Gauging Station	RI	FY^{+}	RI	FY^{+}	RI	FY^{+}	RI	FY^{+}	RI	$FY^{^+}$
Luleälven	Sitasjaure	1.7	68.6	1.5	60.0	1.4	68.6	1.5	65.7	1.4	57.1
	Satihaure	1.6	60.0	3.1	68.6	0.6	62.9	1.8	71.4	2.5	77.1
	Suorva	0.8	54.3	1.3	57.1	1.4	57.1	2.3	65.7	2.7	68.6
	Porjus	1.4	60.0	1.0	57.1	0.8	68.6	0.1	57.1	1.9	65.7
	Messaure	0.3	51.4	1.6	60.0	0.2	60.0	2.3	62.9	0.9	48.6
	Tjaktjajaure	2.2	60.0	1.6	60.0	1.1	57.1	0.9	42.9	1.7	60.0
	Parki	1.2	54.3	1.5	65.7	0.3	51.4	0.4	54.3	1.5	57.1
	Letsi	-0.2	54.3	-0.4	60.0	-0.6	60.0	-0.1	54.3	0.5	54.3
	Boden	1.0	65.7	1.6	57.1	0.1	60.0	-0.6	45.7	2.2	60.0

		Ja	n	Fe	b	М	ar	Α	pr	М	ay
River	Gauging Station	RI	FY^{+}	RI	$FY^{^+}$	RI	FY^{+}	RI	FY^{+}	RI	$FY^{^{+}}$
Skellefteälven	Sädvajaure	-0.2	57.1	1.0	57.1	0.1	54.3	1.4	60.0	1.9	60.0
	Riebnesjaure	0.4	54.3	1.7	62.9	0.2	54.3	0.9	62.9	1.6	57.1
	Hornavan	-0.1	54.3	1.4	62.9	-0.4	60.0	0.6	51.4	0.8	57.1
	Uddjaur-Storavan	0.2	60.0	-1.3	54.3	0.0	60.0	-0.1	57.1	-0.4	57.1
	Bergnäs-Vargfors	0.4	62.9	0.1	57.1	-0.4	54.3	0.6	54.3	-0.8	60.0
	Vargfors-Rengård	-0.7	54.3	-1.3	60.0	-1.2	54.3	-0.8	57.1	0.5	62.9
	Rengård-Kvistfors	1.9	57.1	1.0	60.0	-1.1	48.6	1.6	60.0	1.1	48.6

		Ja	an	Fe	eb	M	ar	Α	pr	М	ay
River	Gauging Station	RI	$FY^{^+}$	RI	$FY^{^{+}}$	RI	FY⁺	RI	FY ⁺	RI	FY [⁺]
Umeälven	Överuman	-0.7	45.7	0.8	60.0	-0.9	51.4	1.9	54.3	1.6	57.1
	Göuta-Ajaure	0.1	51.4	2.0	51.4	1.9	57.1	2.6	54.3	2.6	57.1
	Abelvattnet	-0.4	51.4	1.0	60.0	1.5	62.9	2.7	62.9	2.5	62.9
	Gardiken	9.2	68.6	10.7	77.1	5.7	65.7	4.2	65.7	3.9	65.7
	Storuman	0.2	60.0	-1.5	57.1	-1.0	57.1	-1.0	45.7	0.0	60.0
	Storjuktan	0.3	62.9	0.5	60.0	-0.4	60.0	0.7	51.4	0.4	57.1
	Bålforsen	0.2	57.1	-1.3	51.4	-0.8	54.3	0.2	51.4	-0.6	54.3
	Harrsele	-0.6	48.6	0.4	62.9	-0.0	57.1	1.1	65.7	1.2	65.7
	Laisvall	11.0	62.9	8.4	60.0	6.2	48.6	9.6	51.4	9.8	48.6
	Sorsele	0.8	57.1	2.4	68.6	1.1	60.0	2.1	60.0	2.3	60.0
	Vindeln	1.8	62.9	1.3	57.1	0.3	54.3	1.2	54.3	0.8	57.1
	Stornorrfors	1.3	57.1	1.6	62.9	0.3	57.1	1.6	57.1	1.4	65.7



		Ja	n	Fe	eb	М	ar	A	pr	М	ay
River	Gauging Station	RI	$FY^{^{+}}$								
Ångermanälven	Ransaren	3.7	65.7	4.9	60.0	4.4	62.9	2.5	60.0	2.9	57.1
	Kultsjön	2.9	60.0	3.6	62.9	3.0	62.9	2.0	60.0	3.0	57.1
	Malgomaj	1.7	62.9	1.1	65.7	0.5	57.1	0.3	51.4	0.6	57.1
	Stenkullafors	1.4	62.9	-0.3	57.1	-0.5	51.4	-1.0	57.1	1.2	60.0
	Hällby	11.4	57.1	14.5	60.0	14.8	57.1	12.4	54.3	14.6	57.1
	Lasele	-1.1	34.3	-1.9	48.6	-0.4	60.0	-0.9	48.6	1.2	60.0
	Lövön	1.0	51.4	0.1	57.1	0.3	54.3	1.8	60.0	2.5	74.3
	Rörströmssjön	-0.0	54.3	1.8	65.7	2.2	60.0	3.3	65.7	2.3	57.1
	Borgasjön	2.0	62.9	3.3	65.7	2.3	68.6	3.0	71.4	4.0	62.9
	Dabbsjön	-0.3	51.4	0.1	54.3	0.3	62.9	1.8	54.3	1.1	48.6
	Storsjouten	1.4	57.1	0.6	51.4	-0.0	51.4	1.5	65.7	1.3	54.3
	Korsselet	1.0	54.3	1.4	51.4	0.5	51.4	1.9	54.3	1.1	60.0
	Tåsjön	3.8	71.4	1.1	57.1	0.3	57.1	2.3	71.4	0.8	60.0
	Flåsjön	-1.2	51.4	-1.7	60.0	-0.4	54.3	-0.3	48.6	5.6	48.6
	Lesjön	-4.5	42.9	-4.9	42.9	-4.1	42.9	-2.7	48.6	-1.8	51.4
	Vängelsjön	0.9	54.3	0.5	48.6	0.4	48.6	0.1	40.0	1.7	51.4
	Kilforsen	1.3	62.9	1.7	60.0	1.3	65.7	1.4	57.1	-0.7	54.3
	Ankarvattnet	0.3	57.1	1.6	57.1	2.0	60.0	3.9	60.0	2.2	60.0
	Blåsjön	3.6	60.0	6.1	62.9	4.4	60.0	5.5	60.0	2.7	57.1
	Jormsjön-Kycklingvattnet	5.0	74.3	4.1	74.3	5.3	68.6	4.9	71.4	1.3	62.9
	Limingen	0.0	60.0	2.5	65.7	2.0	65.7	3.3	65.7	1.7	51.4
	Kvarnbergsvattnet	5.2	65.7	4.9	65.7	4.4	71.4	5.2	68.6	3.9	71.4
	Bågede	1.5	54.3	-0.5	57.1	-0.8	45.7	0.5	60.0	1.3	62.9
	Ramsele	12.9	62.9	7.2	65.7	6.5	60.0	5.5	62.9	13.4	57.1
	Hjälta	-1.0	48.6	-5.2	31.4	-3.7	51.4	-6.0	40.0	-1.2	48.6
	Sollefteå	-16.2	48.6	-15.8	48.6	-15.1	48.6	-15.8	48.6	-13.0	42.9

		Ja	ın	Fe	eb	М	ar	A	pr	M	ay
River	Gauging Station	RI	$FY^{^+}$	RI	$FY^{^{+}}$	RI	$FY^{^{+}}$	RI	FY^{+}	RI	FY^{+}
Indalsälven	Torrön	-0.6	57.1	1.8	60.0	0.9	62.9	3.4	71.4	1.6	57.1
	Anjan	1.4	62.9	3.3	62.9	-0.7	60.0	1.5	68.6	0.5	60.0
	Kallsjön	-2.5	54.3	-1.4	51.4	-1.5	54.3	1.0	57.1	1.3	65.7
	Östra Noren	3.9	60.0	4.6	62.9	2.7	65.7	1.7	60.0	1.5	54.3
	Liten	26.3	62.9	25.3	57.1	25.4	65.7	31.8	65.7	34.0	62.9
	Håckren	2.5	60.0	3.2	54.3	0.5	62.9	0.0	57.1	0.4	54.3
	Näkten	-2.2	45.7	-2.0	51.4	-4.8	51.4	-7.1	48.6	-4.7	54.3
	Storsjön	0.4	60.0	-3.3	57.1	-5.3	54.3	-4.8	51.4	-4.3	51.4
	Stora Mjölkvattnet	1.7	60.0	2.7	62.9	1.7	62.9	3.2	82.9	2.8	71.4
	Övre Oldsjön	1.5	62.9	1.9	57.1	1.5	60.0	1.4	57.1	1.9	60.0
	Landösjön	0.4	51.4	0.3	57.1	-0.2	51.4	1.2	54.3	2.1	68.6
	Rörvattnet	3.2	60.0	2.9	60.0	1.8	62.9	0.8	62.9	1.8	60.0
	Rengen	1.8	57.1	1.9	54.3	1.9	60.0	2.1	65.7	2.1	57.1
	Hotagen	8.5	77.1	6.2	74.3	5.7	65.7	6.1	60.0	6.5	57.1
	Midskog	2.7	48.6	3.5	60.0	1.9	48.6	3.5	51.4	3.0	54.3
	Gesunden	3.0	60.0	-2.8	48.6	-9.1	42.9	-0.3	54.3	5.0	62.9
	Hammarforsen	2.7	62.9	2.1	62.9	1.3	54.3	3.3	57.1	5.6	62.9
	Oxsjön	-2.5	45.7	-3.0	54.3	-3.7	54.3	-3.4	45.7	-0.9	48.6
	Bergeforsen	-1.7	65.7	-2.3	68.6	-2.2	68.6	-6.4	60.0	-9.5	57.1



		Jan		Feb		Mar		Apr		May	
River	Gauging Station	RI	$FY^{^+}$	RI	$FY^{^{+}}$	RI	FY^{+}	RI	FY [⁺]	RI	$FY^{^{+}}$
Ljungan	Storsjön	1.7	60.0	2.0	57.1	0.8	57.1	1.0	57.1	1.9	57.1
	Flåsjön	4.7	68.6	3.2	65.7	2.7	65.7	2.3	68.6	1.1	57.1
	Lännässjön	2.1	60.0	-0.4	51.4	-1.8	45.7	-1.9	40.0	-0.5	45.7
	Torpshammar	4.4	54.3	3.1	65.7	1.5	48.6	-0.4	48.6	1.7	54.3
	Viforsen	-1.5	54.3	-5.2	51.4	-6.4	48.6	-6.2	45.7	-0.3	51.4

		Jan		Feb		Mar		Apr		May	
River	Gauging Station	RI	$FY^{^+}$	RI	$FY^{^+}$	RI	$FY^{^{+}}$	RI	$FY^{^{+}}$	RI	$FY^{^{+}}$
Ljusnan	Grundsjön	1.5	54.3	0.9	57.1	0.3	60.0	0.2	51.4	0.9	51.4
	Lossen	1.8	62.9	1.5	62.9	0.6	65.7	0.7	51.4	2.3	62.9
	Lofssjön	-0.3	45.7	0.2	51.4	-0.7	45.7	-1.7	42.9	4.0	65.7
	Svegsjön	1.6	60.0	1.0	54.3	0.0	57.1	-2.1	37.1	1.8	68.6
	Dönje	0.6	62.9	0.6	57.1	0.4	62.9	-4.5	42.9	-0.6	45.7
	Alfta	52.4	71.4	47.4	71.4	51.5	71.4	58.3	74.3	58.6	71.4



HYDROLOGICAL SEASONAL FORECAST SYSTEM

In this project a prototype multi-model system for forecasting the volumes of the spring flood has been developed and evaluated for selected rivers in northern Sweden. On average the Hydrological Seasonal Forecast System (HSFS) performs better than the operational IHMS forecasts 62% of the time which translates to a 2% reduction in the accumulated volume error in the spring flood period across all rivers and forecast dates. It is achieved through combinations of different model chains that employ three different approaches to seasonal forecasting into a multi-model ensemble forecast.

Another step forward in Swedish energy research

Energiforsk – Swedish Energy Research Centre is a research and knowledge based organization that brings together large parts of Swedish research and development on energy. The goal is to increase the efficiency and implementation of scientific results to meet future challenges in the energy sector. We work in a number of research areas such as hydropower, energy gases and liquid automotive fuels, fuel based combined heat and power generation, and energy management in the forest industry. Our mission also includes the generation of knowledge about resource-efficient sourcing of energy in an overall perspective, via its transformation and transmission to its end-use. Read more: www.energiforsk.se

